# *Photocatalytic $CO_2$ valorization by using $TiO_2$, $ZrO_2$ and graphitic based semiconductors*

F. R Pomilla, R. Molinari
Department of Environmental and Chemical Engineering,
University of Calabria, DIATIC
Via Pietro Bucci, 87036 Rende CS, Italy
francescarita.pomilla@unical.it

E. I. García-López, G. Marcì, L. Palmisano
Department of Energy, Information Engineering and Mathematical Models,
University of Palermo, DEIM
Viale delle Scienze, 90128 Palermo, Italy

***Abstract*—In this century, a broad scientific interest has been devoted to fulfill sustainable industrial processes and climatic change remediation. In this prospective, various green technologies have been studied to valorize $CO_2$. The aim of this research is the $CO_2$ reduction in presence of water by using the photocatalytic technology with nanomaterials as the photocatalysts. The present work overviews the main outcomes obtained by using graphitic and oxide based photocatalysts both in gas/solid and liquid/solid batch reactors under simulated solar light. In all gas/solid regime tests the major products detected were methane, carbon monoxide, and acetaldehyde.**

***Keywords—Photocatalysis, $CO_2$ photoreduction, oxides, carbon nitride, graphene, $CO_2$ valorization.***

## I. INTRODUCTION

Catalysis is ubiquitous in the chemical industry and a key technology in a sustainable economy. The progressive substitution of products derived from fossil fuels plays a crucial role to successfully decarbonize industrial processes. In this scenario carbon dioxide ($CO_2$) could be considered as a promising alternative feedstock for chemicals and fuels. The United Nations Framework Convention on Climate Change (UNFCCC) defines the climate change as a weather change due directly or indirectly to human activity, altering the composition of the global atmosphere. From the mid to late 20$^{th}$ century onwards, this phenomenon is largely attributed to the increased levels of atmospheric $CO_2$ produced by the use of fossil fuels. Therefore, a growing scientific interest has been addressed to find a green solution to global heating by reducing the $CO_2$ emissions, and particularly transforming it into chemicals or fuels. Since solar light has been considered as an infinity energy source, the catalysis technology assisted by light (photocatalysis) is a promising green approach to solve different environmental problems, and among them $CO_2$ valorization. The heterogeneous photocatalytic technology is defined as a catalytic process where a semiconductor upon irradiation with energy higher or equal to its band gap ($E_g$) gives rise to a catalized reaction. Photocatalysis is, to all effects, a catalytic process that can be divided into various steps: (i) diffusion of the reactants from the fluid phase to the surface of the catalyst; (ii) adsorption of the reagent(s); (iii) reaction in the adsorbed phase; (iv) desorption and (v) diffusion of the product(s) into the bulk of the fluid phase [1]. Additionally, the fundamental principle in photocatalysis is the promotion of electrons from the valence band (VB) to the conduction band (CB) of the semiconductor, due to absorption of photons with energy equal to or greater than the band gap of the semiconducting photocatalyst. In this way holes ($h^+$) in the VB and electrons ($e^-$) in the CB are produced. These charge carriers can migrate to the surface and initiate a series of chemical reactions with the adsorbed species on the surface of the catalyst. The photogenerated positive holes ($h^+$) can directly react with a substrate to oxidize it or to form strongly oxidizing hydroxyl radicals ($^{\bullet}OH$) in the presence of water. On the other hand, in an aerobic medium electrons could be trapped by oxygen molecules or react with water to form hydroxyl radicals. In an anaerobic medium, instead, they can directly reduce a substrate, as for instance $CO_2$. Recombination of hole and electron pairs is also a possible event which decreases the photo-catalytic efficiency. The main reactions occurring on the semiconductor particle in a generic photocatalytic process are illustrated in Figure 1.

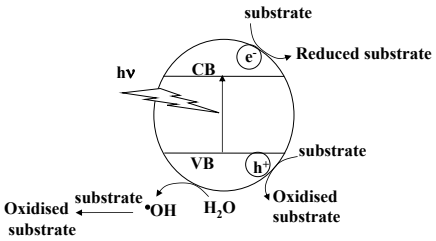


Fig. 1. Mechanism of a generic photocatalytic reaction by using a solid semiconductor as the photocatalyst.

Different semiconductors exhibit various band gap values along with valence and conduction band edges position, so that photo-produced hole/electron pairs show different oxidation and reduction potentials. The band positions for some semiconductors used in heterogeneous photocatalysis are reported in Figure 2. From a thermodynamic point of view, the reduction and oxidation surface reactions can be driven by the photogenerated carriers, $e^-$ and $h^+$, respectively, only when their reduction and oxidation potentials lie between the CB and the VB potentials. The thermodynamic driving forces in photocatalytic processes are strongly dependent on the relative relationships between the CB/VB potentials of the photocatalysts used and the redox potentials of the target reactions. Thus, the more negative the values of the conduction

978-1-5386-6282-3/18/$31.00 ©2018 IEEE

band and the more positive those of the valence band are, the more favoured the reduction and oxidation reactions, respectively. Indeed, as indicated in Figure 2, some semiconductors are more suitable for $CO_2$ reduction (in red).

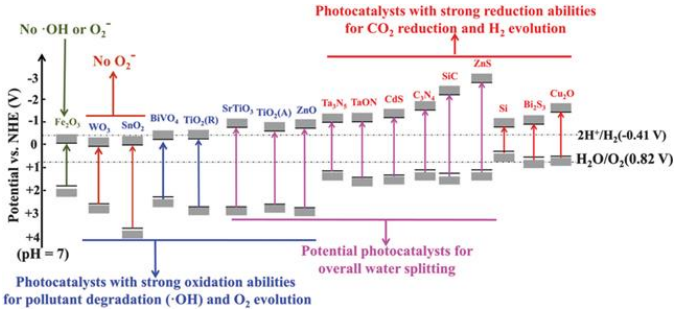


Fig. 2. Band positions and potential applications of some typical photocatalysts at pH 7 in aqueous solutions and versus Normal Hydrogen Electrode (NHE). Reproduced from [2].

The application of photocatalytic reactions to water and air remediation has been widely studied, and $TiO_2$ has represented the most studied semiconductor due to its atoxicity, easy and inexpensive synthesis, appropriate band gap value, high surface area, recyclability, high photoactivity, wide range of processing procedures, and excellent chemical and photochemical stability. However, $TiO_2$ presents some drawbacks, the most important related to its band gap energy (ca. 3.2 eV, for the anatase phase, 3.0 eV. for the rutile phase) which obliges the use of UV light to generate $e^-/h^+$ couples required to start the photocatalytic process. To use sunlight in which, however, only 5% of UV fraction is present, is of course, by far desirable. A plethora of materials has been studied as more sustainable photocatalysts, and among them metal oxides, polymeric or organic type solids, both pristine and as composites, mainly mixed with$TiO_2$. In 1979 Inoue et al. used for the first time the photocatalysis technology to reduce $CO_2$ [3]. They used $TiO_2$, ZnO, CdS, SiC and $WO_3$ in a $CO_2$ saturated aqueous suspension illuminated by a Xe lamp and they found small amounts of formic acid, formaldehyde, methanol and methane. From then, different types of nanostructured semiconductor photocatalysts were used with the aim of optimizing the sustainability of the process (i) by shifting the light absorption ability of the catalyst to the visible part of the solar spectrum, hence rising the photon efficiency of the process and (ii) by decreasing the recombination rate of the photo-produced carriers ($e^-/h^+$). The presence of intermediate states between the VB and CB (doping strategy), or alternatively the formation of a p-n heterojunction between two solids in a nanocomposite, were found also to be good strategies for the enhancement of the performance of the photocatalysts. In the $CO_2$ valorization contest, the assisted use of photocatalytic technology and nanomaterials design, is studied to enhance the $CO_2$ conversion in fuel or added-value molecules.

$CO_2$ reduction is an arduous task, as it is a very stable molecule; indeed its CO bond enthalpy is +805 kJ/mol, so its conversion to light organics requires substantial energy input for the bond cleavage. Mimicking the photosynthesis process by the photocatalytic technology using a solid nanomaterial, appears to be a possible strategy to achieve $CO_2$ conversion. For this aim the main physico-chemical features to consider in order to design an efficient photocatalyst could be (i) the presence of a basic site on the photocatalytic solid surface to allow the adsorption and the destabilization of the $CO_2$ structure (weak acidic molecule) by a geometric distortion, (ii) to select solids with a high surface area (SSA) to increase the number of catalytic sites, (iii) to use photocatalysts with VB and CB values which are compatible with the reduction potential of $CO_2$ (see Figure 2). The solid photocatalysts with more negative CB positions (semiconductors highlighted in red in Figure 2) could produce electrons with enough reduction ability to reduce $CO_2$. Nevertheless, it is worth to remind that the oxidative part of the reaction cannot be neglected. The hole removal is an important step for the success of the overall process, and it has been reported that the hole scavenging rate is the key efficiency-limiting step for the heterogeneous photo-assisted $CO_2$ reduction [4]. Consequently, the optimization of the hole transfer step, for instance by using appropriate electron donors, could improve the efficiency of the process. Many efforts have been focused to design a catalyst able to perform the most sustainable and green approach: the simultaneous $CO_2$ reduction and $H_2O$ oxidation. Photosynthesis of plants generally proceeds in nature according to the so-called Z-scheme, where two independent reactions occur, namely water oxidation and $CO_2$ reduction. Mimicking the natural photosynthesis process, the artificial Z-scheme semiconductor heterojunctions have been successfully proposed by combining two different compounds [5]. When water plays the role of the hole scavenger, its oxidation occurs by following equation (1). (reduction potential = + 0.82 V vs NHE at pH 7, see Figure 2). Water, reacting with the photogenerated hole, provides $H^+$ needed for $CO_2$ reduction reaction, reported in equation (2):

$$2H_2O + 4\ h^+ \rightarrow 4H^+ + O_2 \qquad (1)$$

$$CO_2 + n\ H^+ + n\ e^- \rightarrow \text{organic species} + m\ H_2O \qquad (2)$$

A huge number of publications are devoted to $CO_2$ photo-reduction carried out in the presence of both pristine solids and composite nanomaterials, both in gas-solid and in liquid-solid systems. The aim of the present manuscript is to present the outstanding results in photocatalytic $CO_2$ reduction obtained also by our group mainly in gas-solid regime by using oxide materials based on $TiO_2$ or $ZrO_2$, or alternatively metal free semiconductors based on carbon materials, as carbon nitride ($C_3N_4$) or graphene, both pristine or as composites with $TiO_2$.

The reduction of $CO_2$ requires a more negative energy level of the bottom of the conduction band of the semiconductor than the reduction potential of the various reduction reactions of the $CO_2$ molecule. Thermodynamic data, showing the alignment of the conduction bands of both polymorphs of $TiO_2$, anatase and rutile, along with those of the $C_3N_4$ are reported in Figure 3. By considering these thermodynamic features, an increasing interest has arouse on the use of the metal free $C_3N_4$ semiconductor as photocatalyst for $CO_2$ reduction, using $H_2O$ as the hole scavenger [6]. Most of the literature on $CO_2$ photoreduction has been focused on the use of $TiO_2$ based materials as photocatalysts both in gas-solid or in liquid-solid

regimes [7-8]. Methane and CO are obtained as the major products in the presence of the commercial $TiO_2$ Evonik P25, although small amounts of methanol are also observed.

In gas-solid regime, Akhter et al. found $CH_4$, MeOH and CO production of 10.4, 0.9 and 17.3 μmol/g, respectively, after 5 h under UV irradiation [7], whereas Mele et al. found 131 μmol/g of HCOOH after 8 h of irradiation [8]. Galli et al. have studied the $CO_2$ reduction in liquid-solid regime by using an aqueous suspension of $TiO_2$ maintained at 70 °C and at 7 Bar of $CO_2$ pressure, producing MeOH, HCOOH, CO, $H_2$ and HCHO [9]. Alternative metal oxides were tested in this reaction, in particular, the interest on $ZrO_2$ is due to its acidic-basic surface sites [10-12]. The pioneer study of Sayama et al. on $ZrO_2$ reports the photocatalytic activity of the pristine oxide in liquid-solid regime in the presence of $HCO_3^-$ or $CO_3^{2-}$. The major products detected were $H_2$ and CO, in amounts of 72 to 295 and 0 to 3 $\mu molg^{-1}h^{-1}$, respectively [10]. Wu et al. in a gas-solid regime system in the presence of $ZrO_2$ found only CO (0.51 $\mu molg^{-1}h^{-1}$), however in the presence of $TiO_2$ P25 the products were $CH_4$, $C_2H_6$ and CO, obtained in amount of 4.11, 0.10 and 0.14 $\mu molg^{-1}h^{-1}$, respectively [11]. This study, thus, evidences a lower photoreduction activity of the $ZrO_2$ with respect to $TiO_2$, but a higher selectivity. A recent research by our group confirmed the $ZrO_2$ photoactivity for $CO_2$ reduction in gas-solid regime, obtaining mainly ethanal with traces of methane, methanol, methanal, propanal and propanone [12].

Due to its physico-chemical properties, as aforementioned, increasing interest has been paid in the last years to graphitic catalyst, particularly on $C_3N_4$ and graphene, to perform the photocatalytic $CO_2$ reduction.

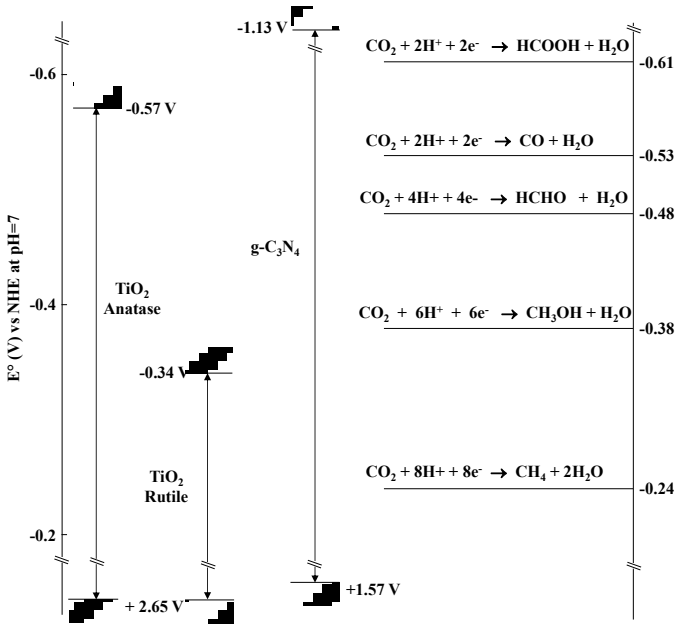


Fig. 3. The redox potentials of the relevant products of $CO_2$ reduction with respect to the estimated position of $TiO_2$, and $C_3N_4$ nanomaterial band edges at pH 7.

The promising photoreduction activity of $C_3N_4$, both pristine and as a composite material, was studied both in gas-solid and liquid-solid regimes [13].

By considering its band gap (c.a. 2.70 eV) and VB and CB edge positions, $C_3N_4$ has been considered an appropriate candidate for photocatalytic water splitting and it has been successively used for photocatalytic decomposition of organic pollutants under visible light. Great attention has been addressed to obtain fuels from $CO_2$ both in gas-solid and liquid-solid regimes. Mao et al obtained methanol and ethanol, 30.2 μmol/g and 21.6 μmol/g, respectively, in liquid-solid regime after 12 h of irradiation by using pristine $C_3N_4$ [14], against the 0.8 μmol/g of methanol reached from Yu et al [15], after 3 h. In order to improve the catalyst efficiency, several attempts have been made. A recent study in gas phase, using a $C_3N_4/TiO_2$ composite reports formation of CO and $CH_4$ in amounts of 6.94 and 1.27 $\mu mol\ g^{-1}\ h^{-1}$, respectively [16]. In addition, a $C_3N_4$-membrane photoreactor to perform $CO_2$ reduction has been also investigated to enhance the reactor efficiency, catalyst stability and production rate [17].

Another interesting graphitic material is graphene (G) which was considered for its electronic properties. This material was first used in composites with $TiO_2$ for $H_2$ production, and recently, the incorporation of these type of carbon nanomaterials to form G-$TiO_2$ nanocomposite photocatalysts has been demonstrated to be suitable for $CO_2$ photoreduction. Tu et al. confirmed the photocatalytic activity of G-$TiO_2$ hybrid materials to convert $CO_2$ into valuable hydrocarbons as $CH_4$ and $C_2H_6$ in the presence of water vapour in gas-solid regime. Notably, the composite with respect to the pristine $TiO_2$ showed an increased activity. No activity was reported for the bare graphene. The weight percentage of graphene in the composite was in the range 1-5 %, and the best results were obtained for the material with the 2% of graphene in $TiO_2$ giving rise to a $CH_4$ and $C_2H_6$ production rate equal to 8 and 16.8 $\mu mol\ g^{-1}\ h^{-1}$, respectively [18]. Liang et al found a higher $CH_4$ production rate with a lower graphene content in the G-$TiO_2$ composite (0.27% of G), although the material was a thin film. They found 8 and 3 $\mu mol\ m^2\ h^{-1}$ of methane by irradiating with UV and Vis light, respectively [19].

The conclusion obtained by studying the literature is that photocatalytic researches on photocatalytic $CO_2$ reduction in gas-solid regime under room conditions report to-date very low production rates of organic products (from $nmolg^{-1}h^{-1}$ to $\mu molg^{-1}h^{-1}$), and only few investigations estimate a production rate in the order of magnitude of $mmolg^{-1}h^{-1}$ [20], but in drastic experimental conditions. To achieve a significant progress by an industrial point of view, the UE program 2020 planned large investments in this field.

## II EXPERIMENTAL SECTION

### *A. Synthesis and characterization of pristine and composite photocatalysts*

Three types of material were prepared in order to use them as photocatalysts in $CO_2$ reduction gas-solid regime: $TiO_2$, $ZrO_2$, both pristine and Ce or Er doped, and $C_3N_4$. Moreover, composites constituted by $C_3N_4$ and $TiO_2$ or graphene and $TiO_2$ were also investigated.

Commercial $TiO_2$ powder Evonik P25 was used along with a home prepared (HP) $TiO_2$ sample, prepared from titanium(IV) chloride ($TiCl_4$, Fluka 98%). The preparation of the HP

material was carried out by slowly adding $TiCl_4$ to distilled water (molar ratio Ti/$H_2O$ 1:60; volume ratio 1:10) at room temperature. After ca. 12 h of continuous stirring a clear solution was obtained. The solution was boiled for 2 h under stirring. This treatment produced a milky white $TiO_2$ dispersion that was dried under vacuum at 323 K.

The oxides based on $ZrO_2$ have been prepared by means of a hydrothermal process, starting from an aqueous solution containing the zirconium precursor which were zirconyl chloride ($ZrOCl_2 \cdot 8H_2O$) or zirconium nitrate ($Zr(NO_3)_4$). A 0.1 M aqueous solution of the precursor was prepared and the pH adjusted to 11 by using 4.0 M NaOH aqueous solution. The suspension was then transferred into a 125 ml Teflon-lined stainless steel autoclave (70% filled), and heated at 175°C overnight. The obtained solid was centrifuged and washed three times with deionized water, dried at 60°C and calcined at 500°C 2 h The final material was $ZrO_2$(Cl) or $ZrO_2$(N) depending upon the precursor. The same procedure described above was followed by adding a Ce or Er salt, ($Ce(SO_4)_2$ or $Er(NO_3)_3 \cdot 5H_2O$) to the 0.1M Zr(IV) containing solution. For each dopant (Ce or Er) four samples with different rare earth (RE) content, 0.5 and 10 % molar percentage were prepared. The $C_3N_4$ metal free photocatalyst was prepared by thermal condensation from melamine [21]. Briefly, 10 g of melamine were put in a covered ceramic crucible and heated at 2 °C $min^{-1}$ up to 520 °C, left for 2 h and slowly cooled down. The obtained solid was powdered, spread on the bottom of a ceramic bowl, calcined at 3 °C $min^{-1}$ up to 520°C, and leaved for 4 h.

Two composites were prepared by using home prepared $C_3N_4$ and $TiO_2$. A planetary mill was used to grind 6 g of Evonik P25 (commercial $TiO_2$) and 2 g of $C_3N_4$ or 5.6 g of $TiO_2$ HP and 2 g of $C_3N_4$. The materials were labelled P25/$C_3N_4$ and HP/$C_3N_4$, respectively. The amount of the two components in the composite derived from their specific surface area (SSA); indeed, quantities corresponding to the same value of SSA were mixed.

In order to prepared the graphene-P25 composite, graphene oxide (GO) was synthesized following the Hummers method [22]. The desired amount of the prepared GO was sonicated for 1 h in a mixture EtOH/$H_2O$ (30 mL + 60 mL) and after the addition of 0.5 g of $TiO_2$ Evonik P25, the suspension was stirred for 1h and hence underwent a hydrothermal treatment for 4 h at 120°C. The final solid was filtered, washed with $H_2O$ and eventually dried at 70 °C overnight. The G/P25 composites contained 0.5, 1, 3, 10 % wt of G with respect to $TiO_2$ P25, and consequently they were labelled as 0.5% G/P25, 1% G/P25, 3% G/P25 and 10% G/P25, respectively.

### *B. Physico-chemical characterization of the powders*

A complete characterization of the pristine and composite materials was performed by using different bulk and surface techniques as X-Ray diffraction (XRD) to analyze the phases present in the samples, diffuse reflectance spectroscopy (DRS) to estimate the optical band gap energy by applying the modified Kubelka Munk function, Raman and FTIR spectroscopies, and specific surface area measurements using the BET model. In some cases photoluminescence or electron paramagnetic resonance (EPR) spectra were recorded. In the latter case also the effect of light (1600 W Mercury/Xenon lamp was used to irradiate the samples) on the spectra was investigated [12].

### *C. Photocatalytic experiments: Gas-solid regime $CO_2$ reduction*

The photocatalytic $CO_2$ reduction was carried out in a cylindrical Pyrex batch photoreactor (V = 25 ml, ø = 45 mm, height = 15 mm) provided with a silicon/teflon septum. 0.06 g of photocatalyst were dispersed in the bottom of the photoreactor. The possible presence of products deriving from C impurities was checked by treating the photocatalysts under irradiation (before the photoactivity experiments in the presence of $CO_2$) with a flow of humid He, which allowed also to clean the surface. Subsequently, the photoreactor was saturated with $CO_2$ containing the vapor pressure of water at 298 K. In order to start the experiment in the presence of humid $CO_2$, the stream of $CO_2$ was continuously flushed at least for 1 h inside the reactor, after bubbling it in a flask containing water. Then the reactor was closed and the lamp was switched on. All of the samples were studied by illuminating the photoreactor, horizontally positioned, by a SOLARBOX apparatus (CO.FO.ME.GRA.), simulating the solar light, equipped with a 1500 W high pressure Xenon lamp. The irradiance reaching the reactor, measured by a Delta Ohm DO 9721 radiometer equipped with a 315-400 nm sensor, resulted 10 and 1000 W/$m^2$ in the range 315-400 nm and 400-950 nm, respectively.

Aliquots of the gaseous reaction mixture were withdrawn at fixed irradiation times by using a gas-tight microsyringe. The evolution of the formed organic products was followed by a GC-2010 Shimadzu equipped with a Phenomenex Zebron Wax-plus column by using He as the carrier gas and a FID. CO was analysed by a HP 6890 GC equipped with a packed column GC 60/80 Carboxen-1000 and a TCD.

## II. RESULTS AND DISCUSSION

### *A. Characterization*

Bare $TiO_2$ HP showed a SSA of ca. 54 $m^2$ $g^{-1}$, close to that of $TiO_2$ Evonik P25 which was 48 $m^2$ $g^{-1}$. The band gaps of these samples were 3.0 and 3.2 eV, respectively [23]. The SSA of $ZrO_2$ was 44 $m^2$ $g^{-1}$, while its band gap ca. 5.0 eV, so this material can be considered as a typical insulator. All of the oxides resulted crystalline, being $TiO_2$ HP (mainly rutile), $ZrO_2$ (ca. 60 % monoclinic, 40 % tetragonal) and $TiO_2$ Evonik P25 (ca. 20% rutile and 80% anatase).

When the $ZrO_2$ material was doped with Ce or Er the formation of intra-band states between the CB and VB enabled its use as photocatalyst. This was justified by the introduction of new electronic states, which modify the optical properties of the $ZrO_2$ giving rise to an active photocatalyst. This phenomenon was more evident by introducing Ce in the $ZrO_2$ crystalline network. Indeed, when Ce was present, the band gap decreased down to 4 eV from 5 eV when 0.5% of Ce was present, and to 3.0 eV in the composite with 10% of Ce. The value of 5.0 eV did not change for all of the composites with

Er. Nevertheless, the presence of increasing amounts of both Ce and Er increased the SSA of the composite material, from 66 to 80 and from 65 to 100 $m^2 g^{-1}$, respectively, for each set of samples containing from 0.5% to 10 % of the rare earth metal. This effect was responsible for the increase of the number of the catalytic sites, the adsorption of reagents, and consequently of the activity.

As far as the metal free $C_3N_4$ semiconductor is concerned, its characteristic structures were confirmed both for the pristine material and for all of the $C_3N_4/TiO_2$ composites, both when HP and commercial P25 $TiO_2$ were used. The XRD analyses showed in the pristine and composite materials the characteristic diffraction peaks of the two components. $C_3N_4$ presents two main peaks at 2θ equal to 13 and 27.4°, relative to intra and inter layer distances. Evonik P25 and home prepared $TiO_2$ showed the characteristic peaks relative to the anatase and rutile phases but, for the last sample broad peaks were observed, indicating a poor crystallinity.

Also FTIR resulted an useful tool to verify the chemical integrity of the 2D metal free semiconductor structure. The pristine $C_3N_4$ showed an FTIR spectrum with bands in the range 870 to 1650 $cm^{-1}$ and 3100 to 3500 $cm^{-1}$. The main peaks attributed to $C_3N_4$ were observed confirming the characteristic structure for the pure and the composite materials. The BET analysis of the $C_3N_4$ powder sample gave a specific surface area of 154 $m^2 g^{-1}$, although this value decreased in the case of the composites.

*B. Photocatalytic $CO_2$ reduction*

Photo-reactivity experiments which were carried out in the presence of pristine $TiO_2$ or $ZrO_2$, Ce and Er doped $ZrO_2$, pristine $C_3N_4$, $C_3N_4/TiO_2$ and $GO/TiO_2$ composites in gas/solid system showed in all cases formation of the same main products, i.e. $CH_4$ and CO, albeit in some cases also acetaldehyde and $CH_3OH$ were also obtained.

In the run carried out in the presence of $TiO_2$ Evonik P25, no product was detected, whilst by using $TiO_2$ home prepared (HP), 0.29 and 1 μmol/g of $CH_4$ and CO, respectively, were found after 6 h of irradiation. The photoactivity of the home prepared $TiO_2$ could be explained by considering the acidic nature of the material, due to the precursor used in the synthesis. Indeed, the powder was prepared in a strong acidic HCl medium, giving to the material Brönsted acidic features which favoured the availability of surface $H^+$ needed for $CO_2$ reduction, as reported in eq. 2.

The $ZrO_2$ pristine material, surprisingly, despite its band-gap value, resulted active and showed higher activity than $TiO_2$ towards $CO_2$ reduction. In particular, during the first 6 h of irradiation, ethanal and traces of methane, methanol, methanal, propanal and propanone were obtained. In all cases, the amount of the organic species increased by increasing the irradiation time, and ethanal was always the major product. The maximum amount of ethanal obtained was ca. 15 μmol $g^{-1}$ and 25 μmol $g^{-1}$ after 6 h and 24 h of irradiation, respectively. Doping with Ce and Er gave rise also to active materials, although the difference between the two metals was negligible. Table 1 reports the amount of products obtained with bare and Ce or Er doped $ZrO_2$ oxides. In some cases CO was obtained, being ca. 35 μmol $g^{-1}$ the maximum amount formed (see Table 1) [12]. The unusual photoactivity of $ZrO_2$ could be explained with the formation of intra band allowing an electronic "double jump" able to photo activate the surface. In particular, the intra band formation was more efficient in the bare catalyst, which showed an increased photo-reducing capacity.

TABLE I. CONCENTRATION OF THE FORMED SPECIES IN THE PHOTOCATALYTIC $CO_2$ REDUCTION AFTER 24 HOURS OF IRRADIATION IN THE PRESENCE OF PRISTINE $ZrO_2$ AND Ce OR Er DOPED $ZrO_2$ BASED MATERIALS

| | *Organic intermediate species [μmol $g^{-1}$]* | | | | | | |
|---|---|---|---|---|---|---|---|
| ***Sample*** | Ethanale | $CH_4$ | $CH_3OH$ | $CH_2O$ | propanal | $CH_3COCH_3$ | CO |
| $ZrO_2$(Cl) | 24.4 | 1.6 | 1.5 | - | 0.2 | 0.4 | 5.0 |
| $ZrO_2$(N) | 44.2 | 4.8 | 3.2 | - | 0.7 | 3.3 | 35 |
| $ZrO_2$(Cl)-Ce0.5% | 8.0 | 0.3 | 0.3 | - | 0.1 | 0.1 | 2.8 |
| $ZrO_2$(N)-Ce10% | 5.6 | 0.3 | 0.3 | - | 0.1 | 0.2 | - |
| $ZrO_2$(Cl)-Er0.5% | 10.0 | 1.0 | 0.6 | 2.0 | 0.2 | 0.4 | 6.0 |
| $ZrO_2$(N)-Er10% | 18.6 | 2.3 | 1.8 | 4.4 | 0.3 | 1.0 | 9.0 |

Experiments carried out by using the graphitic materials showed different products distribution. In the presence of pristine $C_3N_4$ photocatalyst, the major products obtained were CO and $CH_4$, 1.54 and 0.43 μmol $g^{-1}$, respectively, after 6 h of irradiation time. To enhance the activity of pristine $C_3N_4$, some tests were carried out with $C_3N_4/TiO_2$ P25 and $C_3N_4/TiO_2$ HP composites. The first one showed a lower $CO_2$ conversion but a total selectivity toward CO, whilst no activity was detected in the presence of $C_3N_4/TiO_2$ HP. We hypothesize that the contemporaneous presence of $C_3N_4$ and $TiO_2$ HP gave rise to neutralization of the acidic sites of the home prepared $TiO_2$ with the basic sites present on the surface of the $C_3N_4$ material, reducing the availability of $H^+$ for the reaction (eq. 2) and reducing also the basic sites necessary for the $CO_2$ adsorption. The main results obtained in the presence of $TiO_2$, $C_3N_4$ and their composites are summarized in Figure 4.

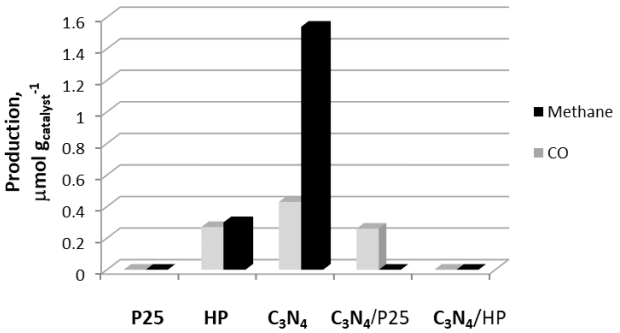


Figure 4. Production of CO and $CH_4$ by using $TiO_2$, $C_3N_4$ and $C_3N_4/TiO_2$ composites after 6 hours of irradiation.

The $CO_2$ photocatalytic reduction experiments carried out in the presence of the binary materials consisting of graphene

and $TiO_2$ Evonik P25 showed the best results among all the tested photocatalysts. The main products, in all cases were $CH_4$, CO and $CH_3OH$. Acetaldehyde was also found in the presence of the 0.5 and 1% G/P25 composites. Results reported in Figure 5 evidence that the 1% G/P25 photocatalyst exhibited the best total carbon converted which was equal to ca. 44 μmol $g^{-1}h^{-1}$.

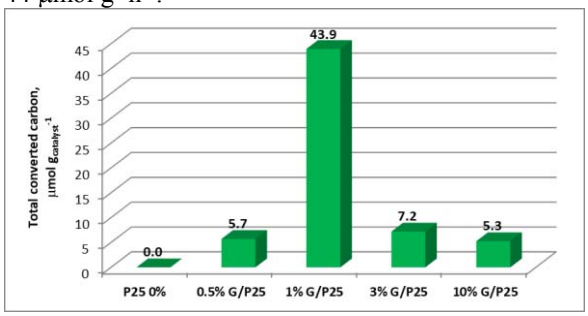


Figure 5. Total carbon converted expressed as μmol $g^{-1}$ $h^{-1}$, estimated as total moles of C in each product obtained, for all graphene composites.

The 1% G/P25 photocatalyst showed a selectivity in $CH_4$, acetaldehyde, MeOH and CO equal to 57, 28, 10 and 6 %, respectively, after 6 h of irradiation time. Thus, by increasing the graphene percentage in the composite, a decrease in the total carbon converted was observed, but at the same time an increase in the selectivity of the process occurred. In particular, after 6 h of irradiation by using the 3% G/P25 photocatalyst, the selectivity towards $CH_4$ was ca. 75%, whilst both $CH_4$ and CO were detected by using the 10% G/P25, with selectivity of 57 and 43 % , respectively.

The most active G/P25 composite (1%G/P25) was also tested in liquid-solid regime in the presence of $HCO_3^-$ (basic pH) with no other hole scavenger different from water, but no product was detected. Whilst, when the experiment was carried out in the presence of $Na_2SO_3$ as hole trap traces of $H_2$ were detected after 6 h.

## REFERENCES


[1] J. M. Thomas, W. J. Thomas, "Principles and Practice of Heterogeneous Catalysis" Wiley, 1996.

[2] L. Xin, Y. Jiaguo, M. Jaroniec, "Hierarchical photocatalysts" Chem. Soc. Rev., 45, 2603-2636, 2016.

[3] T. Inoue, A. Fujishima, S. Konishi, K. Honda, "Photoelectrocatalytic reduction of carbon dioxide in acqueous suspensions of semiconductor powders" Nature, 1979, 277, 637.

[4] K. Wu, Z. Chen, H. Lv, H. Zhu, C. L. Hill and T. Lian, "Hole removal rate limits Photodriven $H_2$ generation efficiency in CdS-Pt and CdSe/CdS-Pt semiconductor nanorod–metal tip heterostructures" J. Am. Chem. Soc., 136, 7708–7716, 2014.

[5] P. Zhou, J. Yu, M. Jaroniec, "All-solid-state Z-scheme photocatalytic systems" Adv. Mater., 26, 4920-4935, 2014.

[6] J. Low, J. Yu, W. Ho, "Graphene-Based Photocatalysts for $CO_2$ Reduction to Solar Fuel" J. Phys. Chem. Lett., 6, 4244−4251, 2015.

[7] P. Akhter, M. Hussain, G. Saracco, N. Russo, "Novel nanostructured-$TiO_2$ materials for the photocatalytic reduction of $CO_2$ greenhouse gas to hydrocarbons and syngas" Fuel, 149, 55–65, 2015.

[8] G. Mele, C. Annese, L. D'Accolti, A. De Riccardis, C. Fusco, L. Palmisano, A. Scarlino, G. Vasapollo, "Photoreduction of carbon dioxide to formic acid in aqueous Suspension: A comparison between Phthalocyanine/$TiO_2$ and Porphyrin/$TiO_2$ catalysed processes" Molecules, 20, 396-415, 2015.

[9] F. Galli, M. Compagnoni, D. Vitali, C. Pirola, C. L. Bianchi, A. Villa, L. Prati, I. Rossetti., "$CO_2$ photoreduction at high pressure to both gas and liquid productsover titanium dioxide" Appl. Catal. B, 200, 386–391, 2017.

[10] K. Sayama and H. Arakawa, "Photocatalytic Decomposition of Water and Photocatalytic Reduction of Carbon Dioxide over $ZrO_2$ Catalyst" J. Phys. Chem., 97, 531-533, 1993.

[11] C.-C. Lo, C.-H. Hung, C.-S. Yuana, J.-F. Wu, "Photoreduction of carbon dioxide with $H_2$ and $H_2O$ over $TiO_2$ and $ZrO_2$ in a circulated photocatalytic reactor" Solar Energy Mater. Sol. Cell,. 91, 1765–1774, 2007.

[12] E.I. García-López, G. Marcì, F.R. Pomilla, M.C. Paganini, C. Gionco, E. Giamello, L. Palmisano, "$ZrO_2$ Based materials as photocatalysts for 2-propanol oxidation by using UV and solar light irradiation and tests for $CO_2$ reduction" Catal. Today, *in press*.

[13] J. Wen, J. Xie, X. Chen, X. Li, "A review on g-$C_3N_4$-based photocatalysts" Appl. Surf. Sci., 39, 72-123, 2017.

[14] J. Mao, T. Peng, X. Zhang, K. Li, L. Ye, L. Zan, "Effect of graphitic carbon nitride microstructures on the activity and selectivity of photocatalytic $CO_2$ reduction under visible light" Catal. Sci. Technol., 3, 1253–1260, 2013.

[15] K. Wang, Q. Li, B. Liu, B. Cheng, W. Ho, J. Yu, "Sulfur-doped g-$C_3N_4$ with enhanced photocatalytic $CO_2$-reduction performance". Appl. Catal. B 176, 44–52, 2015.

[16] K. Li, B. Peng, J. Jin, L. Zan, T. Peng, "Carbon nitride nanodots decorated brookite $TiO_2$ quasi nanocubes for enhanced activity and selectivity of visible-light-driven $CO_2$ reduction" Appl. Catal. B, 203, 910–916, 2017.

[17] F. R. Pomilla, A. Brunetti, G. Marcì, E.I. García-López, E. Fontananova, L. Palmisano, G. Barbieri, "$CO_2$ to liquid fuels: photocatalytic conversion in a continuous membrane reactor" *Submitted*.

[18] W. Tu, Y. Zhou, Qi Liu , S. Yan , S. Bao , X. Wang, M. Xiao, and Z. Zou, "An in situ simultaneous reduction-hydrolysis technique for fabrication of $TiO_2$-graphene 2D sandwich-like hybrid nanosheets: graphene-promoted selectivity of photocatalytic-driven hydrogenation and coupling of $CO_2$ into methane and ethane". Adv. Funct. Mater., 23, 1743–1749, 2013.

[19] Y. T. Liang, B. K. Vijayan, K. A. Gray, M. C. Hersam, "Minimizing Graphene Defects Enhances Titania Nanocomposite-Based Photocatalytic Reduction of $CO_2$ for Improved Solar Fuel Production". Nano Lett., 11, 2865–2870, 2011.

[20] Z. Zhao, J. Fan, J. Wang, R. Li, "Effect of heating temperature on photocatalytic reduction of $CO_2$ by N–$TiO_2$ nanotube catalyst". Catal. Commun., 21, 32–37, 2012.

[21] I. Krivstov, E.I. García-López, G. Marcì, L. Palmisano, Z. Amghouz, J.R. García, S. Ordóñez, E. Díaz, "Selective photocatalytic oxidation of 5-hydroxymethyl-2-furfural to2,5-furandicarboxyaldehyde in aqueous suspension of g-$C_3N_4$" Appl. Catal. B, 204, 430-439, 2017.

[22] W. S. Hummers, R. E. J. Offeman, "Preparation of Graphitic Oxide" J. Am. Chem. Soc., 80, 1333-1339, 1958.

[23] M. Bellardita, A. Di Paola, E. García-López, V. Loddo, G. Marcì, L. Palmisano, " Photocatalytic $CO_2$ Reduction in Gas-Solid Regime in the Presence of Bare, $SiO_2$ Supported or Cu-Loaded $TiO_2$ Samples" Curr. Org. Chem., 17, 2440-2448, 2013.